Accepted Manuscript

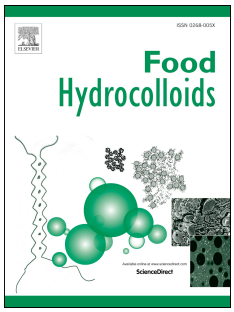

Mechanical properties of bacterial cellulose synthesised by diverse strains of the genus *Komagataeibacter*

Si-Qian Chen, Patricia Lopez-Sanchez, Dongjie Wang, Deirdre Mikkelsen, Michael J. Gidley

PII: S0268-005X(17)31582-5

DOI: 10.1016/j.foodhyd.2018.02.031

Reference: FOOHYD 4290

To appear in: *Food Hydrocolloids*

Received Date: 29 September 2017

Revised Date: 22 December 2017

Accepted Date: 18 February 2018

Please cite this article as: Chen, S.-Q., Lopez-Sanchez, P., Wang, D., Mikkelsen, D., Gidley, M.J., Mechanical properties of bacterial cellulose synthesised by diverse strains of the genus *Komagataeibacter*, *Food Hydrocolloids* (2018), doi: 10.1016/j.foodhyd.2018.02.031.

Diverse mechanical properties of bacterial cellulose hydrogels determined by cellulose concentration and fibril architecture

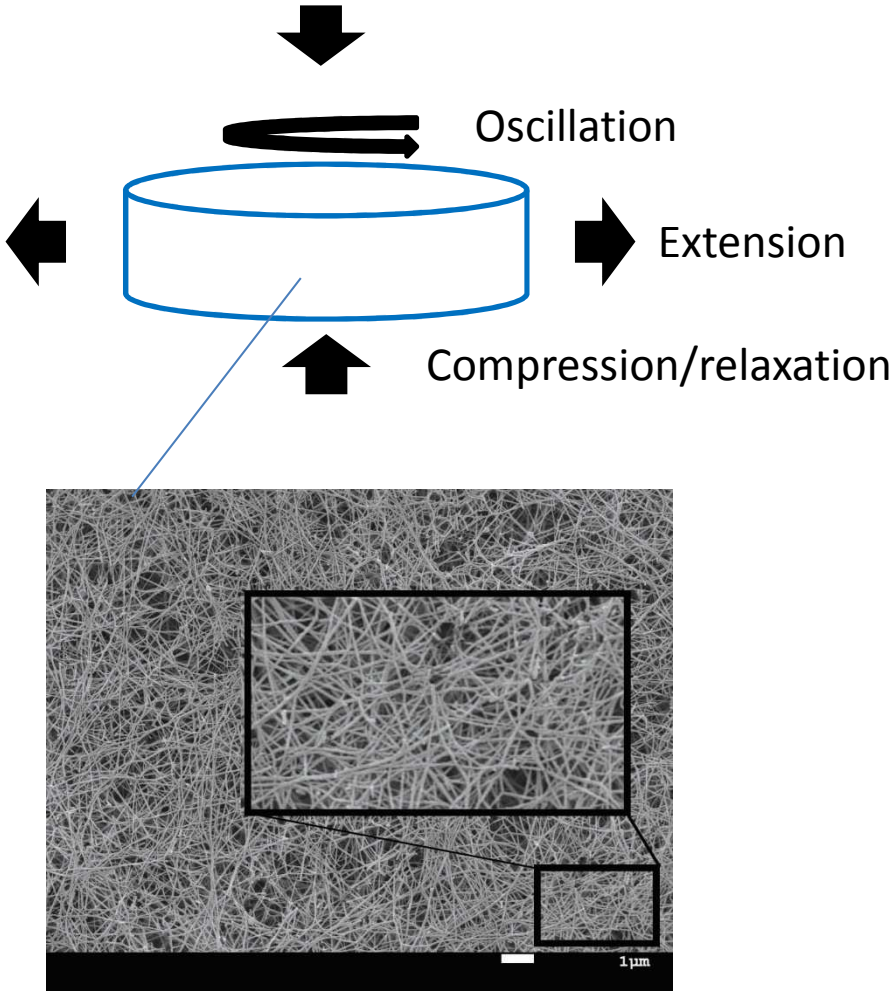

Mechanical properties of Bacterial Cellulose Synthesised by Diverse Strains of the Genus *Komagataeibacter*

Si-Qian Chen[1], Patricia Lopez-Sanchez[1], Dongjie Wang[1, #], Deirdre Mikkelsen[1] and Michael J Gidley[1*]

[1] ARC Centre of Excellence in Plant Cell Walls, Centre for Nutrition and Food Sciences, Queensland Alliance for Agriculture and Food Innovation, The University of Queensland, St. Lucia, Brisbane, QLD 4072 (Australia).

[#] Current address: Tianjin University of Science and Technology, College of Food Engineering and Biotechnology, No. 29, 13th. Avenue, Tianjin Economic and Technological Development Area (TEDA), Tianjin, China, 300457

[*] Corresponding author. Phone: +61 7 3365 2145. Email address: m.gidley@uq.edu.au (M. J. Gidley)

Abstract

Bacterial cellulose (BC) has several current and potential future uses in the food industry because of its ability to form hydrogels with distinctive properties. The texture of BC hydrogels is determined by both the cellulose fibre network and the internal dispersed water. In this study, mechanical properties of hydrated BC synthesised by six different strains of *Komagataeibacter* genus were investigated with regards to their extensibility, compressive strength, relaxation ability, viscoelasticity and poroelasticity. The stress/strain at failure and Young's modulus were assessed by uniaxial tensile testing. The compressive strength, relaxation ability and viscoelasticity were measured via a series of compression and small amplitude oscillatory shear steps. A poroelastic constitutive modelling simulation was used to investigate the mechanical effects of water movement. The morphology of the BC fibril network under compression was observed via scanning electron microscopy. Results showed that the mechanics of BC were highly dependent on the cellulose concentration, as well as the morphology of the fibril network. BC synthesised by ATCC 53524 was the most concentrated (0.71 wt%), and exhibited high tensile properties, stiffness and storage moduli; whereas the comparatively low mechanical properties were noted for BC produced by ATCC 700178 and ATCC 10245, which contained the lowest cellulose concentration (0.18 wt%). Small deformation responses (normal stress, G') scaled with cellulose concentration for all samples, whereas larger deformation responses (Young's modulus, poroelasticity) depended on both cellulose concentration and additional factors, presumably related to network morphology. Increasing concentration and compressive coalescence of fibres in the integrated BC network reduced both the relaxation of the normal stress and the movement of water. This research aids the selection of bacterial strains to modulate the texture and mechanical properties of hydrated BC-based food systems.

Keywords bacterial cellulose hydrogel; tensile test; compression test; small amplitude oscillatory rheology; poroelasticity

1. Introduction

The interest in cellulose as an important source of food structuring and insoluble dietary fibre has increased for both the food industry and consumers over the past decade. Food gels based on cellulose, like *Nata-de-coco*, are valued for their juicy mouthfeel and chewable texture (Zhang et al., 2017). The *Nata-de-coco* is derived from fermentation of certain bacterial strains which produces ultra-fine fibres of bacterial cellulose (BC) in the form of a hydrogel. BC hydrogels are characterised by a randomly oriented three-dimensional swollen fibril network (typically above 99 wt% water). The chemical structure of BC is identical to plant cellulose, i.e. β-1-4-linked glucan chains. These chains are arranged into relatively crystalline BC fibres (also called ribbons), containing a large amount of hydroxyl groups on their surfaces. Recent X-ray and neutron scattering analyses suggest that BC fibres have a core-shell structure built up from microfibril units of *ca*. 3.4 nm diameter (Martínez-Sanz et al., 2016). The microfibrils coalesce with the inclusion of some water molecules to eventually become long fibres/ribbons with a diameter of 10-130 nm (Martínez-Sanz et al., 2016), and these apparently randomly oriented ribbons form a highly hydrated gel in the aqueous fermentation conditions.

This ultrastructure determines the unique mechanical properties of BC including high water-holding capacity, good extensibility, viscoelasticity and poroelasticity (Keshk & Sameshima, 2006; Martínez-Sanz et al., 2015). Generally, BC hydrogels are able to hold 100-200 times their own weight of water (Lin et al., 2009). In a previous report, the hydrated BC exhibited an apparent Young's modulus as high as 14.2 MPa and a breaking strength up to 2.2 MPa under uniaxial tensile testing (McKenna et al., 2009). In addition, BC hydrogels follow typical viscoelastic and poroelastic behaviour, determined by both the porous network itself and the dynamics of water within the hydrogel (Lopez-Sanchez et al., 2014); these factors are relevant for textural properties such as juiciness, chewiness and gumminess. Due to these characteristics, BC has been used in a range of food products and in other applications (Ullah et al., 2016). However, a deeper understanding of the mechanics of BC hydrogels is required to optimise textural properties and to explore novel applications of BC in the food industry.

Generally, BC-producing bacteria include the genera *Agrobacterium*, *Aerobacter*, *Achromobacter*, *Azotobacter*, *Komagataeibacter* (formerly *Gluconacetobacter*), *Rhizobium*, *Sarcina*, and *Salmonella* (Shoda & Sugano, 2005). Compared with other genera, the *Komagataeibacter* genus generally has higher BC yield and purity, and therefore is usually selected for research purposes and food production (Ruka et al., 2012). Screening for high

BC yield *Komagataeibacter* mutants is the objective of many investigations (Castro et al., 2012; Ha & Park, 2012; Ishikawa et al., 2014; Son et al., 2003; Watanabe et al., 1998). However, the mechanical property differences between BC hydrogels produced by many different strains of the *Komagataeibacter* genus have not previously been reported.

In this study, five commonly used commercial *Komagataeibacter* strains and one experimental strain were selected. *Komagataeibacter xylinus* ATCC 10245 and *Komagataeibacter xylinus* ATCC 53524 have been widely used to prepare BC/hemicellulose and BC/pectin composites as cell wall analogues (Astley et al., 2001; Astley et al., 2003; Chanliaud et al., 2002; Mikkelsen et al., 2015; Tokoh et al., 2002; Whitney et al., 1999). *Komagataeibacter xylinus* ATCC 700178 (formerly *Acetobacter xylinum* subsp. *sucrofermentas* BPR2001) is able to synthesise spherical shaped BC in an agitating environment (Hiroshi et al., 1995). The tensile properties of dehydrated BC and BC/Poly (L-lactic) acid composites produced by *Komagataeibacter xylinus* NBRC 13693 have been previously studied (Quero et al., 2010). *Komagataeibacter hansenii* ATCC 23769 is also a commonly used cellulose-producing strain in research on the physical properties of BC (Brown et al., 2011). Additionally, an experimental strain, *Komagataeibacter xylinus* KTH 5655, was also included. We have recently reported that KTH 5655 can produce more ordered crystalline BC (Chen et al., 2017), which may influence its mechanical properties.

The extensibility, stiffness and viscoelasticity of BC produced by these six microbial strains were compared using uniaxial tensile testing, compression-relaxation and small amplitude oscillatory shear (SAOS). The experimental data obtained from compression-relaxation was used to fit a theoretical model to derive parameters determining poroelastic behaviour, i.e. how the mechanical properties of the network are coupled with fluid flow within it. In addition, the structural changes of BC at different stages of compression were observed via scanning electron microscopy (SEM) to investigate the relation between fibre morphology and mechanics. Mechanical and rheological properties were analysed in terms of cellulose concentrations and microstructure of the BC hydrogels.

2. Materials and methods

2.1. Preparation of BC hydrogels

Bacterial strains *Komagataeibacter xylinus* ATCC 53524, *Komagataeibacter xylinus* ATCC 10245, *Komagataeibacter hansenii* ATCC 23769 and *Komagataeibacter xylinus* ATCC 700178 were sourced from the American Type Culture Collection (Manassas, VA,

USA). *Komagataeibacter xylinus* NBRC 13693 was from the Biological Resource Centre (Kisarazu-shi, Chiba, JAP). *Komagataeibacter xylinus* KTH 5655 was kindly provided by the Division of Glycoscience, School of Biotechnology, Royal Institute of Technology (Stockholm, Sweden).

The fermentation process followed the method previously described (Chen et al., 2017). All bacterial strains were grown at 30 °C, pH 5.0, in Hestrin and Schramm (HS) agar medium (20 g/l glucose, 5 g/l peptone, 5 g/l yeast extract, 2.7 g/l Na_2HPO_4, 1.15 g/l critic acid) for 3 days. The colonies were then transferred into HS broth medium for a further 3 days, before being shaken at 150 rpm for 5 minutes to release attached cells from the gels. The released cells were then transferred to a scaled-up incubation broth, making up a 10 wt% inoculation, and fermented for 3 days in a 40 mm diameter cylinder shape container. Post-fermentation, the harvested hydrogels were washed in ice-cold autoclaved milliQ water under gentle agitation.

2.2 Cellulose concentration, density and water holding capacity (WHC) of BC

The weight of harvested BC hydrogels was measured before and after being air-dried in an oven at 105 °C for 48 hours. The BC concentration (wt%) was calculated as dry weight divided by weight of the hydrated gel. The density was defined as the dry weight divided by the volume of the hydrogel. The WHC was defined as the total water content divided by the dry weight. Three replicates were measured.

2.3 Scanning electron microscopy (SEM)

BC samples for SEM were prepared by using freeze substitution followed by critical point drying (Autosamdri-815, Tousimis, Rockville, Maryland 20852, USA) to replace the water following a series of dehydration steps (Lopez-Sanchez et al., 2015). After drying, samples were coated with 10 nm of iridium (Bal-tec coater, Leica microsystems, Wetzlar, Germany) and examined using a JSM 7100F SEM (JEOL, Tokyo, Japan) at 5kV and 10 mm working distance. Images were taken from at least three different positions for each sample at increasing magnifications (from ×1000, ×5000, ×10000, and × 25000 to × 50000).

2.4 Uniaxial tensile testing

Tensile tests of BC hydrogels were conducted by using an Instron 5543 machine (Instron, Melbourne, Australia). Each pellicle was cut into three dumbbell shaped strips (end

dimensions: 6×35 mm; narrow section dimensions: 2×10 mm) using a dumbbell press (ISO 37-4) (Fig. 1). The thickness of the strip was measured using a digital calliper. The two ends of the strip were placed between the vice grips, and were moved apart at a constant speed of 10 mm/min. A 5 N load cell was used and the force required for extension as a function of time was recorded. The tensile stress (MPa) and strain at the breaking point of the strip were recorded. The apparent Young's modulus (MPa) was defined by the slope of the linear region of the strain-stress curve during the stretching stage. At least twelve replicates were conducted for each sample.

a) **b)**

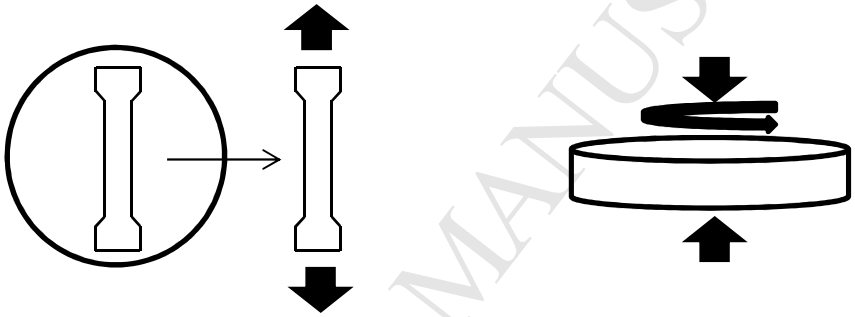

Fig. 1 Schematic representation of (a) the tensile testing of a dumbbell shaped sample cut parallel to the surface of a BC pellicle and (b) the compression and oscillation of a BC pellicle.

2.5 Small amplitude oscillatory shear (SAOS)

Frequency sweep tests were conducted at frequencies ranging from 0.1 rad/s to 100 rad/s. Before the test, BC hydrogels were compressed to 0.8 mm to have the same initial thickness, and the diameter was measured by using a digital calliper. The shear stress was set at 1 Pa following a previously published method (Lopez-Sanchez et al., 2015). The test was carried out on a rotational rheometer (HAAKE Mars III Rheometer, Thermo Fisher Scientific, Karlsruhe, Germany) at 25 °C controlled by a Peltier device. Emery paper (P240/S85, 58 μm roughness) coated parallel titanium plates (60 mm diameter) were used (Davies & Stokes, 2005).

2.6 Cycle test: compression and SAOS

The cycle test used in this study has been previously described (Lopez-Sanchez et al., 2014). The combination of compression and oscillation steps in a single test gives the possibility to follow viscoelastic properties as a function of concentration in the same sample. In addition, during the oscillatory test the recovery of the normal force was recorded making it possible to study sample relaxation. In the compression test, the initial gap between the two plates was set to be the same as the height of the gels, measured with a calliper. The BC hydrogels were compressed by moving the upper plate at a 1 μm/s constant speed downwards (Fig. 1). The normal force of the hydrogel was recorded by a normal force transducer (50 N). The normal stress at each compression stage was divided by the initial value for normalisation. Every 100 μm, the compressing force was removed and the sample was allowed to relax and the normal force recovery recorded during 180 s. Samples were eventually compressed to a thickness of 0.5 mm after a series of compression-oscillation cycles. At least three replicates were tested.

The SAOS test was conducted on the same samples after each compression step. The storage (G') and loss moduli (G'') were recorded. Frequency was set to 1 Hz with a shear stress of 1Pa.

The Poisson's ratio (υ) was calculated for each hydrogel from

$$\upsilon = - d\varepsilon_{radial}/d\varepsilon_{axial}$$

where ε_{radial} and ε_{axial} represent the radial and axial strain after compression.

2.7 Poroelastic behaviour and linear transversely poroelastic model

Experimental data for BC hydrogels from the compression/relaxation test was used to fit a transversely isotropic biphasic model (Cohen et al., 1998; Lopez-Sanchez et al., 2014). The axial modulus, radial modulus and permeability (*k*) were obtained and compared for the different BC hydrogels. The fitting process of experimental data with the poroelastic model was conducted in Matlab (version: R2015a) (Bonilla et al., 2016).

2.8 Statistical analysis

One-way ANOVA ($p=0.05$) was used to determine the statistical differences of concentration, density, WHC, breaking stress/strain and Young's modulus for BC hydrogels synthesised by different *Komagataeibacter* strains. All the statistical analyses were conducted by using R scripts (version 3.2.3) in RStudio.

3. Results and discussion

3.1. Cellulose concentration, density and WHC of BC hydrogels

Table 1 summarises the water content and cellulose concentrations of BC synthesised by the six *Komagataeibacter* strains. The concentrations of BC in the hydrogels produced by NBRC 13693, ATCC 53524 and KTH 5655 (0.60%, 0.72% and 0.42% respectively) were higher than BC produced by ATCC 700178, ATCC 10245 and ATCC 23769 (0.19%, 0.18% and 0.22% respectively). The density was consistent with the cellulose concentration. This result is in line with the BC yields data previously reported (Chen et al., 2017). The variation of concentration and density was also reflected in the appearance of the hydrogels (supplementary material Fig. 1). BC hydrogels produced by NBRC 13693, ATCC 53524 and KTH 5655 appeared homogenously opaque, whilst gels synthesised by ATCC 700178, ATCC 10245 and ATCC 23769 were more heterogeneous and contained transparent sections. Previous reports have correlated transparency of dehydrated BC films with their cellulose concentration (Quero et al., 2010).

Table 1 Cellulose concentration, density and WHC of BC hydrogels produced by different strains.

Bacterial strain	Cellulose concentration (wt%)	Density (g/cm^3)	WHC (%)
ATCC 700178	0.19 ± 0.1^{e}	0.0024 ± 0.001^{e}	$(5.26 \pm 0.35)\times10^{4\,a}$
ATCC 10245	0.18 ± 0.1^{e}	0.0024 ± 0.001^{e}	$(5.44 \pm 0.27)\times10^{4\,a}$
ATCC 23769	0.22 ± 0.1^{d}	0.0031 ± 0.001^{d}	$(4.50 \pm 0.20)\times10^{4\,b}$
NBRC 13693	0.6 ± 0.1^{b}	0.0069 ± 0.001^{b}	$(1.65 \pm 0.15)\times10^{4\,d}$
ATCC 53524	0.72 ± 0.1^{a}	0.01 ± 0.002^{a}	$(1.37 \pm 0.11)\times10^{4\,e}$
KTH 5655	0.42 ± 0.1^{c}	0.0045 ± 0.001^{c}	$(2.35 \pm 0.18)\times10^{4\,c}$

Additionally, the WHC for the hydrogels was associated with the cellulose concentration. For less concentrated gels, each gram of cellulose was able to hold more water than the highly-concentrated gels. The amount of liquid in cellulosic hydrogels contributes to the aroma and flavour release of jelly desert products like *Nata-de-coco* (Budhiono et al., 1999). However, the concentration of cellulose also influences the texture of BC hydrogels (Jagannath et al., 2011). Hence, selecting an appropriate *Komagataeibacter* strain could be used to achieve a desired balance between liquid release and texture for BC hydrogel products.

3.2 Tensile properties of BC hydrogels

Uniaxial tensile testing (Fig. 2a) showed that BC hydrogels produced by different *Komagataeibacter* strains displayed overall viscoelastic behaviour during stretching. In the low strain region (0 to 0.025), applied stress was less dependent on the tensile strain. This was followed by a near linear plastic region (0.025 to 0.15) until the stress was sufficient to break the sample when the strain was above approximately 0.15. The linear plastic region was used to calculate the apparent Young's modulus (Drury et al., 2004).

In general, the BC hydrogels produced by NBRC 13693, ATCC 53524 and KTH 5655 had significantly higher breaking stress (0.62 MPa, 0.68 MPa and 0.62 MPa respectively) than the gels from ATCC 700178, ATCC 10245 and ATCC 23769 (0.15 MPa, 0.36 MPa and 0.12 MPa respectively) in line with their relative cellulose concentrations (Table 1 & 2). Also, the apparent Young's modulus was dependent on the concentration, with the values for BC from NBRC 13693, ATCC 53524 and KTH 5655 (3.08 MPa, 5.56 MPa and 3.83 MPa respectively) being higher than for BC from ATCC 700178, ATCC 10245 and ATCC 23769 (1.10 MPa, 2.87 MPa and 1.26 MPa respectively). Stress to break also correlated with the cellulose concentration, with more concentrated samples exhibiting higher breaking stress. However, the breaking strains for different BC were similar, ranging from 16% to 20%. Similar results were found for BC harvested after long-term fermentation. A longer fermentation period (9 days) increased the cellulose concentration in the gel (supplementary material Fig. 2) compared with those harvested after a shorter fermentation period (3 days) (Fig. 2a). However, the BC from NBRC 13693, ATCC 53524 and KTH 5655 still contained more cellulose and showed higher tensile stress and Young's modulus than BC produced by ATCC 700178, ATCC 10245 and ATCC 23769.

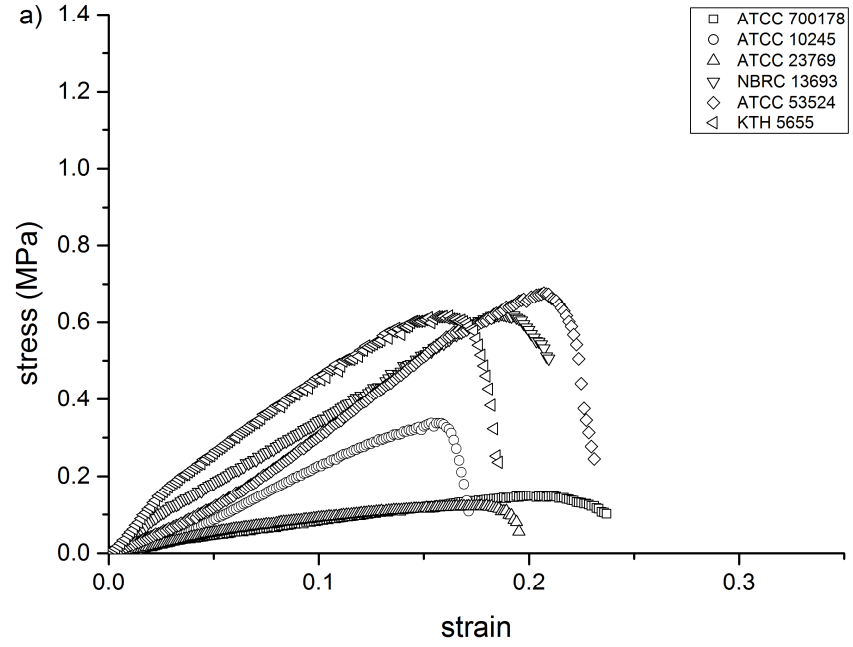

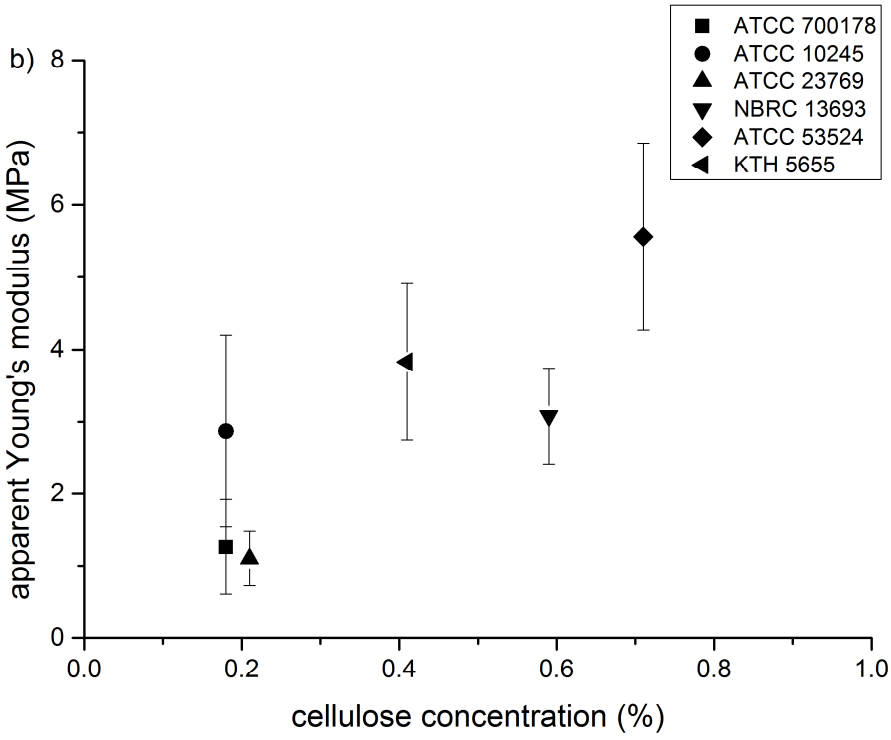

Fig. 2 Representative stress/strain curves (a) and apparent Young's modulus as a function of cellulose concentration (b) generated during tensile testing of BC hydrogels synthesised by different *Komagataeibacter* strains.

253 **Table 2 Tensile testing characteristics of BC produced by six different strains.**

Bacterial strain	Breaking stress (MPa)	Breaking strain (%)	Apparent Young's modulus (MPa)
ATCC 700178	0.15 ± 0.08^{c}	20.72 ± 8.32^{a}	1.10 ± 0.38^{d}
ATCC 10245	0.36 ± 0.08^{b}	18.60 ± 8.03^{a}	2.87 ± 1.33^{c}
ATCC 23769	0.12 ± 0.04^{c}	17.97 ± 5.04^{a}	1.26 ± 0.66^{d}
NBRC 13693	0.62 ± 0.17^{a}	18.69 ± 3.25^{a}	3.08 ± 0.66^{c}
ATCC 53524	0.68 ± 0.13^{a}	20.72 ± 6.03^{a}	5.56 ± 2.29^{a}
KTH 5655	0.62 ± 0.16^{a}	16.20 ± 2.91^{a}	3.83 ± 1.08^{b}

254 Different superscripts in each column denote significant ($p<0.05$) value differences

255

256 During tensile testing of hydrogels, the initial stretching process alters the polymer
257 network configuration and polymer-water interactions (Drury et al., 2004). Previously we
258 found that both the crystallisation and average diameters of the ribbons were similar for all
259 these BC materials (Chen et al., 2017). It has also been shown that ordered alignment of
260 fibres should reduce the resistance for deformation, but an isotropic fibril network would
261 effectively enhance the stiffness of the gel (McKenna et al., 2009). Hence, cellulose
262 concentration and fibre orientation are expected to be the most significant structural factors
263 affecting tensile properties. Diverse bacterial strains producing different cellulose
264 concentrations under the fermentation conditions used, result in different apparent Young's
265 modulus values for BC hydrogels (Fig, 2b). Although the greater density of ribbons present at
266 higher concentrations contributed to the high Young's modulus, it was not a strict linear
267 correlation. This is probably due to network structural variations of the different BC materials.
268 BC hydrogels contain anisotropic features due to their laminated architecture on the 10-100
269 μm length scale, containing cellulose ribbon-rich layers and ribbon-depleted gaps between
270 the layers (Buyanov et al., 2010; Lopez-Sanchez et al., 2015; Nakayama et al., 2004). During
271 the fermentation process, it has been suggested that newly produced ribbons are added into
272 the layer until it is completed (Hu et al., 2014), but it is not understood what determines the

size of layers. These layers would likely become aligned parallel to the direction of stretching under tension, and the constituent ribbons would straighten and eventually break (McKenna et al., 2009). Therefore, these structural variations can be regarded as a secondary factor which influence the tensile properties of BC from different strains and worthy of further investigation.

3.3 Mechanical properties when BC hydrogels are under compression

A recent report showed that the Poisson's ratio of BC hydrogels synthesised by ATCC 53524 was near zero, indicating insignificant radial expansion during normal compression (Lopez-Sanchez et al., 2014). Here, it was found that BC gels produced by the other five strains (NBRC 13693, ATCC 53524, KTH 5655, ATCC 23769 and ATCC 10245) also essentially maintained their original diameters after compression (final thickness = 0.5 mm), with Poisson ratio values all below 0.03 $\pm$0.01. Generally, porous materials like cork can have zero values of Poisson's ratio, which is determined by the foldable open-cell alveolar architecture (Greaves et al., 2011). The honeycomb-like structure bends and buckles under the external axial force, leading to a near zero radial extension (Fortes & Teresa Nogueira, 1989). This behaviour is likely to be explained by the previously described laminated microstructure of the BC, i.e. fluid is expressed from between layers on compression rather than requiring radial deformation of individual layers.

Under compression, the normal stress was defined as the normal force from the BC hydrogels against the upper plates divided by its surface area (approximately 13 cm^2). The apparent axial modulus was defined as the linear slope of the normal stress-strain curves at large strains. It was found that both the normal force and apparent axial modulus rose with the process of compression (Fig. 3a). The hydrogel produced by ATCC 53524 had the highest normal stress (4800 Pa) when it reached the maximum compression strain, compared with the BC from the other five strains. Comparatively, the gel produced by ATCC 700178 had the lowest normal stresses (120 Pa). Additionally, the axial modulus of the BC produced by ATCC 53524 was also the highest (10 kPa to 100 kPa) when the strain was above 0.4, which means it was approximately 10 times stiffer than the gel produced by ATCC 700178 at the same strain.

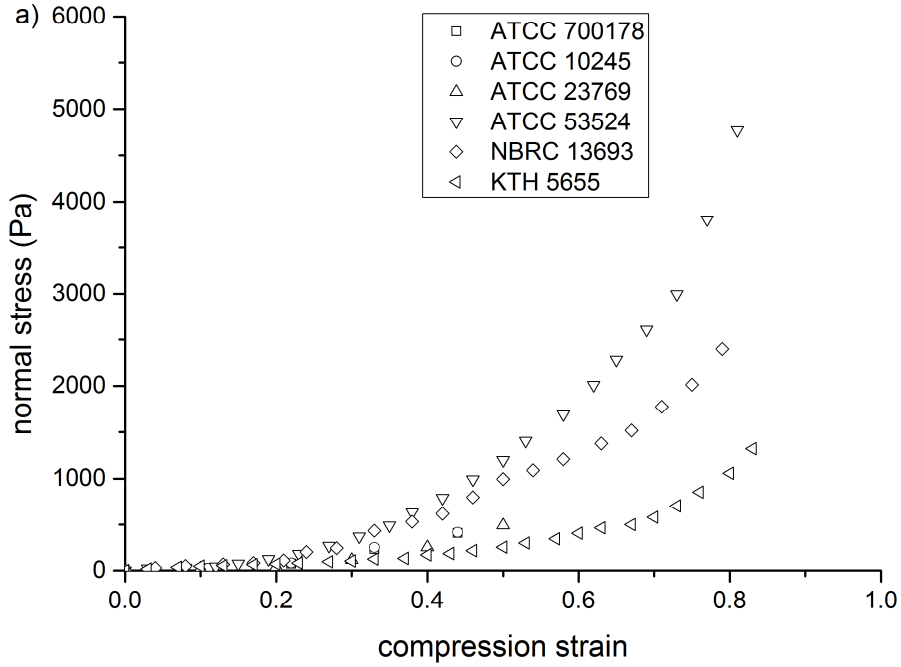

302

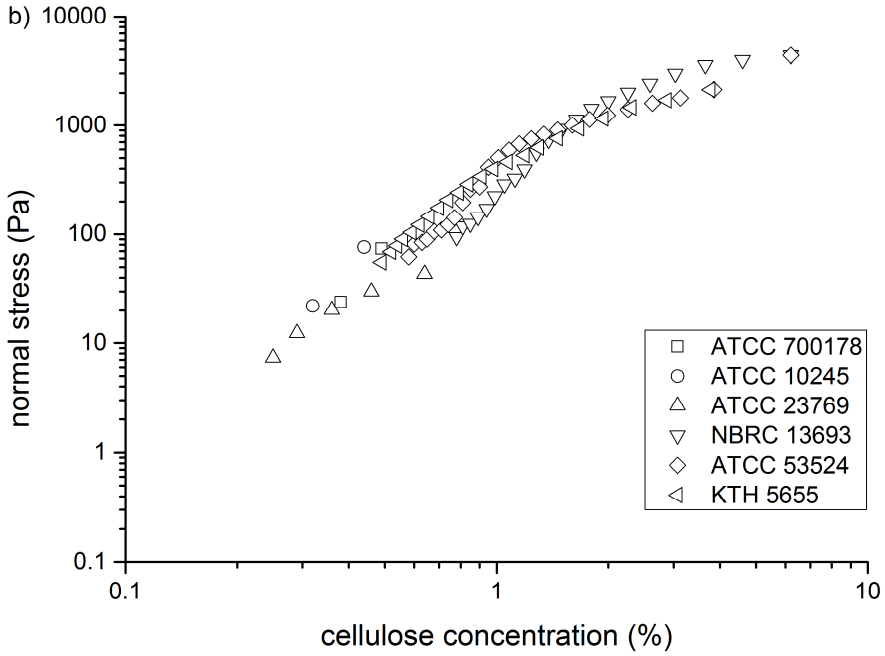

303

304 **Fig. 3 Representative normal stress-strain curves (a) and representative normal stress-**
305 **cellulose concentration curves (b) generated during compression tests of BC hydrogels**
306 **from diverse *Komagataeibacter* strains.**

307

It is likely that the concentration of BC significantly contributed to the mechanical properties under compression. The dependence of cellulose concentration *vs* normal stress for BC produced by the six strains is shown in Fig.3b. Overall, all BC hydrogels followed a similar increasing tendency of normal stress with increasing cellulose concentration under compression, which included a marked increase of stress at low concentrations (<2%), with less dependence at higher concentrations with a tendency towards a plateau.

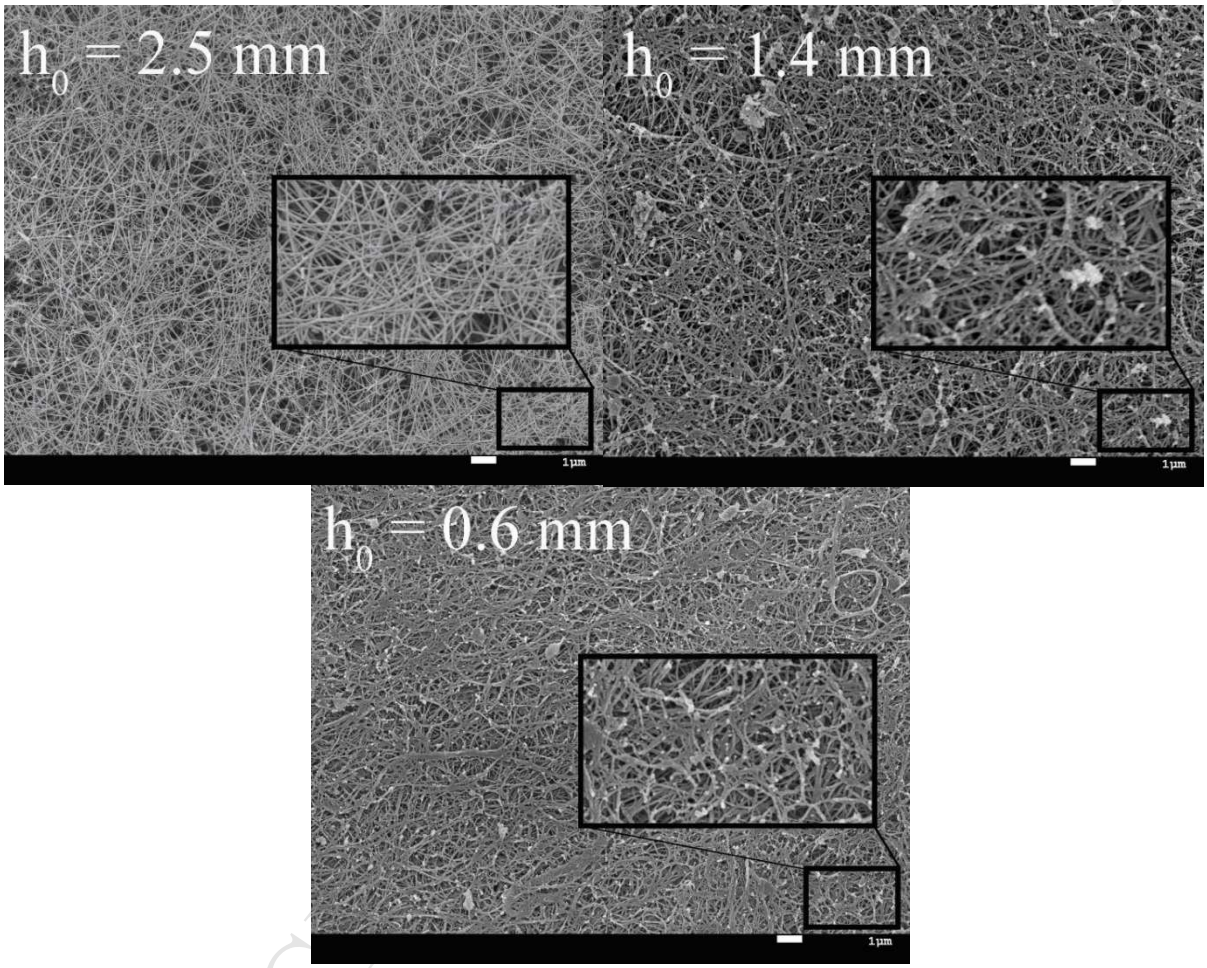

Fig. 4 SEM images of BC network produced by KTH 5655 at different thickness of gels, before and after compression from an original thickness of 2.5 mm, with insert magnified images showing BC ribbons (scale bar = 1 µm).

In general, the stiffness of BC depends on the cellulose concentration, as well as the structure of the fibril network. During compression, water was gradually squeezed out of the porous hydrogels, which increased contacts between the fibres and enhanced the stiffness. In addition, the structural alteration of the fibril network also contributed to its mechanical properties. The morphology of BC hydrogels produced by KTH 5655 at different thicknesses

during compression is shown in Fig. 4. For the uncompressed sample (h_0 = 2.5 mm), the fibril network was spongy and porous, and the individual rod-shape ribbons can be observed. When the gel was compressed to a thickness of 1.4 mm, the fibres started to entangle with each other, and the density of the network was increased. After the gel was compressed to 0.6 mm, more aggregated fibres were observed, and they lost their original features, appearing to have coalesced. This reinforcement of the network density increased the stiffness.

3.4 Compression-relaxation and poroelastic characteristics of BC hydrogels

The relaxation behaviours of BC hydrogels were determined from the recovery of normal stress when the external normal force was removed. Due to the limited initial thickness of BC produced by ATCC 700178, ATCC 10245 and ATCC 23769, only the samples of two different thicknesses produced by ATCC 53524, NBRC 13693 and KTH 5655 were analysed. The recovery of normal stress in BC hydrogels after compression from 1.4 to 1.3 mm was compared with that after compression at higher cellulose concentration (from 0.6 to 0.5 mm).

Overall, BC hydrogels exhibited two distinct regions during the compression process including a viscoelastic region at low strain rate (< 0.25), followed by an apparently plastic deformation region at high strain rate (0.25 to 0.1). When the compression was stopped, all gels showed time-dependent relaxation behaviour, during which the normal force initially dropped rapidly and then reached a slow-decreasing plateau. Specifically, during the large gap (h=1.4 mm) compression (Fig. 5a), the hydrogel produced by ATCC 53524 reached the highest normal stress (1213 Pa) compared with NBRC 13693 (786 Pa) and KTH 5655 (573 Pa), which correlated with the concentration of cellulose (2.4%, 1.6% and 1.3% respectively). Also, the axial modulus of gel from ATCC 53524 was approximately 2 times higher than the modulus of gels produced by NBRC 13693 and KTH 5655. When the gels were compressed to 0.6 mm of thickness, the concentrations of ATCC 53524, NBRC 13693 and KTH 5655 were boosted to 6.8%, 3.8% and 2.9% respectively. The normal stress of BC produced by ATCC 53524 increased to 4357 Pa (Fig. 5b), which was almost twice that of NBRC 13693 (1876 Pa) and KTH 5655 (1567 Pa). Additionally, the variation of axial modulus was also enlarged when the concentration increased. The BC produced by ATCC 53524 showed approximately 4 times higher modulus than that gel from NBRC 13693 and KTH 5655.

353 The relaxation ability of BC hydrogels was also associated with their cellulose
354 concentration. When the thickness was 1.4 mm, even after the gel had been relaxed for a long
355 period, the gel produced by ATCC 53524 did not recover its original stiffness, whereas gels

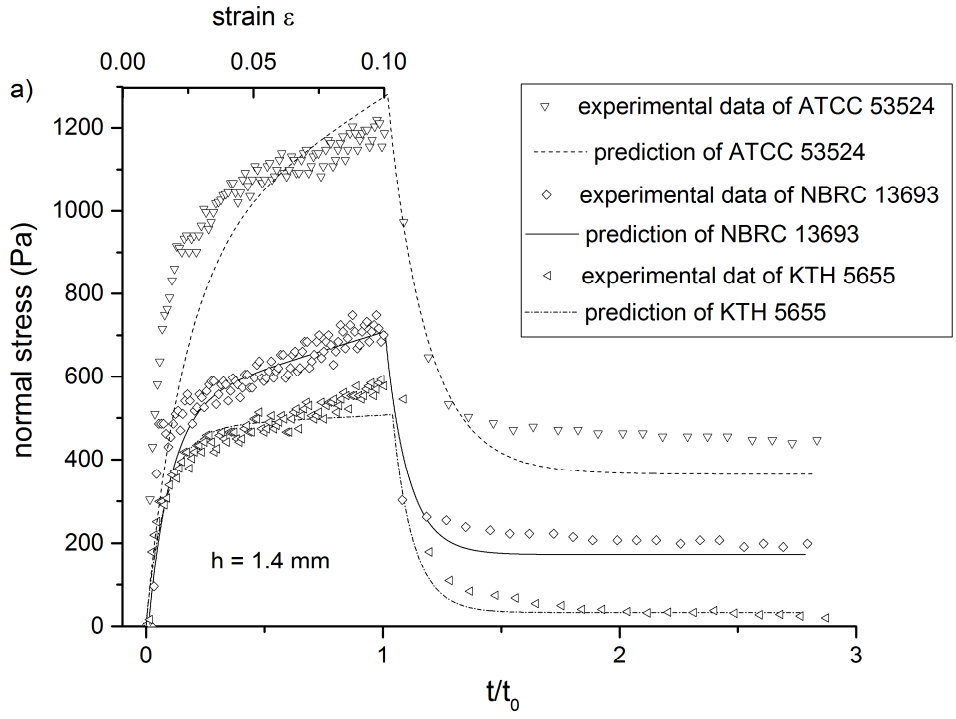

356

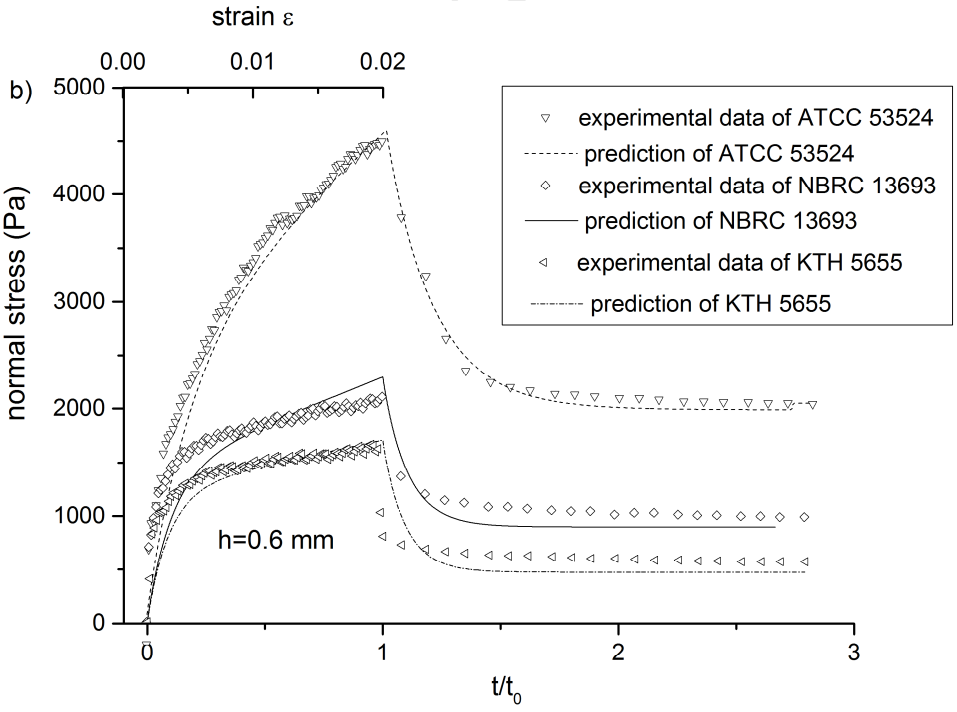

357

Fig. 5 Representative compression-relaxation for BC hydrogels produced by ATCC 53524, NBRC 13693 and KTH 5655 for thicknesses of (a) 1.4 mm and (b) 0.6 mm. The compression stage occurs for t/t_0 from 0 to 1, followed by relaxation. The experimental data is presented as open symbols, while the lines represent fitting of the data with the poroelastic model.

from NBRC 13693 and KTH 5655 exhibited more complete relaxation. When the gels were compressed to 0.6 mm of thickness, the relaxation ability of the BC produced by these three different strains was decreased, especially for the gel produced by ATCC 53524 which had the highest BC concentration. For each hydrogel, the relaxation ability was dependent on the morphology of the fibril network. As shown in Fig. 4, the fibril network twisted and the ribbons lost their original rod-shape in the more compressed BC hydrogels, consistent with a reduction of mechanical relaxation ability.

By fitting the experimental data with a linear transversely poroelastic model, further mechanical parameters were estimated including the axial modulus, radial modulus and permeability (Table 3). Essentially, the axial modulus obtained by the fitting with the model was consistent with the experimental results. Additionally, the modulus of BC produced by ATCC 53524 was higher than NBRC 13693 and KTH 5655, and this variation was enlarged for the more compressed samples, which subsequently cause variation in cellulose concentration. The model also provided information on the permeability of BC materials, which is a key factor for the mouthfeel of BC-based food products. The hydrogel produced by ATCC 53524, which also contained the highest amount of cellulose, showed the lowest permeability (2.9×10^{-14} m^2) when it was compressed to 0.6 mm thickness. Comparatively, the BC of 1.4 mm thickness produced by KTH 5655 had the highest permeability (7.6×10^{-14} m^2). The relatively 'open' structure of the less concentrated gel was easier for water diffusion, especially for the uncompressed hydrogels. Based on the SEM images (Fig. 4), for the uncompressed samples, several large and clear pores between ribbons in the BC gel are observed. In the more compressed samples, both the sizes and numbers of pores were decreased. Due to the porous structure of BC hydrogels, it was assumed that the movement of water in the cellulose matrix would follow Darcy's law, as is the case for some other poroelastic materials (Argoubi & Shirazi-Adl, 1996). With the increasing level of fibre aggregation and decreasing pore size during compression, the permeability should reduce accordingly.

Table 3 Mechanical parameters of different BC hydrogels of 1.4 mm and 0.6 mm thickness. The axial modulus, radial modulus and permeability were obtained through fitting of the experimental data with the poroelastic model.

	Concentration (%)		Peak normal stress (Pa)		Axial modulus (kPa)		Permeability $k \times 10^{-14}$ (m^2)	
Strain	1.4 mm	0.6 mm	1.4 mm	0.6 mm	1.4 mm	0.6 mm	1.4 mm	0.6 mm
ATCC 53524	2.4	6.8	1213	4357	5.1	12.5	3.9	2.9
NBRC 13693	1.6	3.8	786	1876	2.4	5.3	6.7	5.9
KTH 5655	1.3	2.9	573	1567	0.4	2.8	7.6	6.7

3.5 Viscoelastic behaviours of BC hydrogels

The viscoelasticity of BC hydrogels produced by different strains of the genus *Komagataeibacter* was investigated via a SAOS test. For all the BC hydrogels, moduli weakly depended on frequency in the test (supplementary material Fig. 3). In this frequency sweep test, all the hydrogels were compressed to an initial thickness of 0.8 mm, so their cellulose concentration varied. The BC produced by ATCC 53524, which had the highest cellulose concentration, showed the highest modulus compared with the BC produced by the other five strains. Moreover, the moduli kept on increasing during the compression (supplementary materials Fig. 4), which also supported the importance of cellulose concentration as a determining factor. It has previously been proposed that in oscillation, the storage modulus depends on the density of fibre entanglements in BC hydrogels (Whitney et al., 1999). The cellulose fibres in highly-concentrated BC gels enlarged the number of

entanglements and led to a high G' value. In addition, for the same sample, their storage modulus (G') always remained higher than the loss modulus (G''), which means all the BC hydrogels produced by different *Komagataeibacter* strains exhibited more elastic behaviour than viscous characteristics, even though all hydrogels contained more than 99% water. This was reflected in the tan δ values of the six types of BC hydrogels, which were all below 0.2 in the SAOS test (supplementary material Fig. 5).

To further understand the relation between elasticity and cellulose concentration, the storage modulus (G') was plotted as a function of cellulose concentration (Fig. 6). Overall, the storage moduli were enhanced when the concentration increased for all six types of BC. The number of fibre entanglements increased markedly at comparatively low cellulose concentration level, and reached a plateau presumably due to the limit where fibres were crushed into each other. At low concentrations there was a clear separation into two behaviour types, in line with the cellulose concentration in pellicles (Table 1). Cellulose from strains which produce low concentration pellicles (700178, 10245, 23769) had greater moduli at concentrations below about 0.8% than the other three higher concentration pellicles, but at concentrations above 1%, there was much less difference. In order to normalise the modulus data to take account of the different starting concentrations in pellicles, the experimental data were fitted with the cascade model, a method used to describe the dependence of the structure of the gel with its concentration (Clark et al., 1989; Clark & Ross-Murphy, 1985; Stokes, 2012) relative to incipient gelling concentration (C_0) for each strain – 0.16,0.17, 0.20, 0.34, 0.40 and 0.45% for 700178, 10254, 23769, 5655, 13693 and 53524 respectively. The experimental data

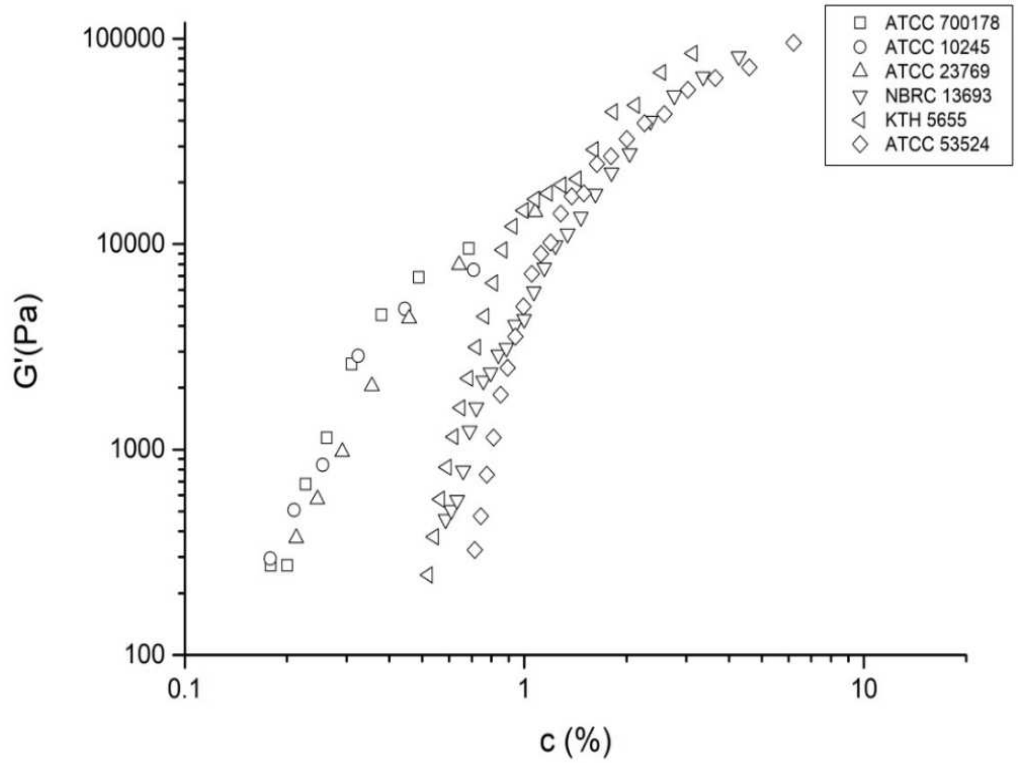

431

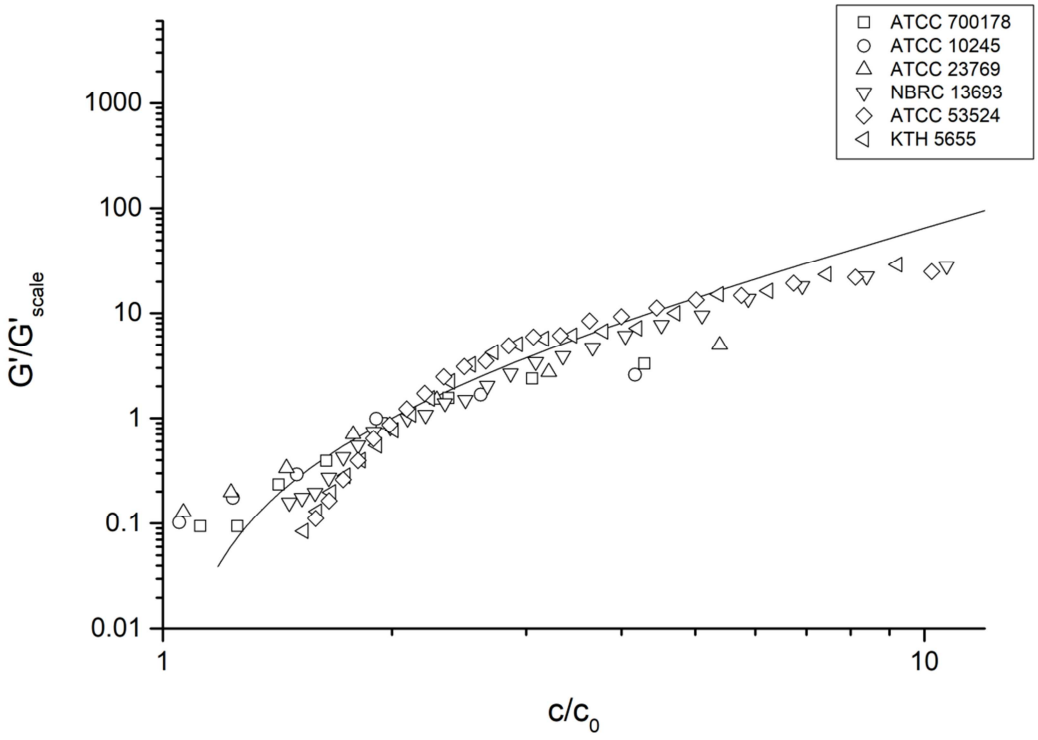

432

433 **Fig. 6 Elastic modulus G' as a function of cellulose concentration (upper graph) and**
434 **scaled elastic modulus G'/G'$_{scale}$ vs scaled concentration c/c$_0$ (lower graph). Open**

symbols represent experimental data. The solid line is the best fit of the data with the cascade model.

followed the equation: G'/G' scale $=(c/c_0 - 1)^n$. In this test, the G'_{scale} was set arbitrarily as 2900 Pa, and for BC material from the different strains, the best fitting exponent n ranged from 1.8 to 1.9. This exponent is similar to $n = 2$, which was found to be the optimum for other biopolymer networks such as agar and carrageenan (Stokes, 2012). Thus the same cross-linking model that is used for interpreting mechanical properties of polysaccharide gels can be applied to cellulose systems that are structured through entanglement of fibres. This analysis indicated that under small deformation oscillatory conditions, the BC hydrogels produced by different *Komagataeibacter* strains exhibit similar mechanical behaviours at the same cellulose concentration.

4. Conclusions

BC hydrogels produced by different strains of the genus *Komagataeibacter* showed diverse mechanical properties in terms of their tensile properties, stiffness, viscoelasticity, porosity and permeability, which depended on both the concentration of cellulose, as well as the structure of the fibril network. Those mechanical features that respond primarily to the number of effective cross-links in the network (normal stress, G') scaled with cellulose concentration for all bacterial strains. Cellulose concentration was also important for larger deformation mechanical features related to network re-organisation (Young's modulus, fluid flow), but additional factors were characteristic of bacterial strain origin, presumably reflecting different network architectures. Mechanical properties can also be tailored by post-synthesis compression to control both stiffness and water movement. Ultimately, this research which has provided detailed structural and mechanical information on BC hydrogels produced by different *Komagataeibacter* strains, may allow the characteristic textural properties to be rationalised and subsequently aid selection of cellulose-producing bacterial strains for biotechnological and food industry application purposes.

Funding

This work was supported by the Australian Research Council Centre of Excellence in Plant Cell Walls [CE110010007] and a studentship to SC from the China Scholarship Council and The University of Queensland.

Acknowledgements

The authors would like to thank Prof. Vincent Bulone for providing strain KTH 5655 and Dr Mauricio Rincon Bonilla for the poroelastic model.

References

Argoubi M, & Shirazi-Adl A (1996) Poroelastic creep response analysis of a lumbar motion segment in compression. *Journal of Biomechanics* 29:1331-1339

Astley OM, Chanliaud E, Donald AM, & Gidley MJ (2001) Structure of *Acetobacter* cellulose composites in the hydrated state. *International Journal of Biological Macromolecules* 29:193-202

Astley OM, Chanliaud E, Donald AM, & Gidley MJ (2003) Tensile deformation of bacterial cellulose composites. *International Journal of Biological Macromolecules* 32:28-35

Bonilla MR, Lopez-Sanchez P, Gidley MJ, & Stokes JR (2016) Micromechanical model of biphasic biomaterials with internal adhesion: Application to nanocellulose hydrogel composites. *Acta Biomaterialia* 29:149-60

Brown EE, Zhang J, & Laborie M-PG (2011) Never-dried bacterial cellulose/fibrin composites: preparation, morphology and mechanical properties. *Cellulose* 18:631-641

Budhiono A, Rosidi B, Taher H, & Iguchi M (1999) Kinetic aspects of bacterial cellulose formation in *nata-de-coco* culture system. *Carbohydrate Polymers* 40:137-143

Buyanov AL, Gofman IV, Revel'skaya LG, Khripunov AK, & Tkachenko AA (2010) Anisotropic swelling and mechanical behavior of composite bacterial cellulose-poly(acrylamide or acrylamide-sodium acrylate) hydrogels. *Journal of the Mechanical Behavior of Biomedical Materials* 3:102-11

Castro C, Zuluaga R, Alvarez C, Putaux JL, Caro G, Rojas OJ, Mondragon I, & Ganan P (2012) Bacterial cellulose produced by a new acid-resistant strain of *Gluconacetobacter* genus. *Carbohydrate Polymers* 89:1033-7

Chanliaud E, Burrows K, Jeronimidis G, & Gidley MJ (2002) Mechanical properties of primary plant cell wall analogues. *Planta* 215:989-996

Chen S-Q, Mikkelsen D, Lopez-Sanchez P, Wang D, Martinez-Sanz M, Gilbert EP, Flanagan BM, & Gidley MJ (2017) Characterisation of bacterial cellulose from diverse *Komagataeibacter* strains and their application to construct plant cell wall analogues. *Cellulose* 24:1211-1226

Clark AH, Gidley MJ, Richardson RK, & Ross-Murphy SB (1989) Rheological studies of aqueous amylose gels: the effect of chain length and concentration on gel modulus. *Macromolecules* 22:346-351

Clark AH, & Ross-Murphy SB (1985) The concentration dependence of biopolymer gel modulus. *British Polymer Journal* 17:164-168

505 Cohen B, Lai WM, & Mow VC (1998) A transversely isotropic biphasic model for
506 unconfined compression of growth plate and chondroepiphysis. *Journal of*
507 *Biomechanical Engineering* 120:491-496
508 Davies GA, & Stokes JR (2005) On the gap error in parallel plate rheometry that arises from
509 the presence of air when zeroing the gap. *Journal of Rheology* 49:919
510 Drury JL, Dennis RG, & Mooney DJ (2004) The tensile properties of alginate hydrogels.
511 *Biomaterials* 25:3187-3199
512 Fortes MA, & Teresa Nogueira M (1989) The poison effect in cork. *Materials Science and*
513 *Engineering: A* 122:227-232
514 Greaves GN, Greer AL, Lakes RS, & Rouxel T (2011) Poisson's ratio and modern materials.
515 *Nature Materials* 10:823-37
516 Ha JH, & Park JK (2012) Improvement of bacterial cellulose production in *Acetobacter*
517 *xylinum* using byproduct produced by *Gluconacetobacter hansenii*. *Korean Journal of*
518 *Chemical Engineering* 29:563-566
519 Hiroshi T, Takaaki N, Akira S, Masanobu M, Takayasu T, & Fumihiro Y (1995) Screening of
520 bacterial cellulose-producing *Acetobacter* strains suitable for agitated culture.
521 *Bioscience, biotechnology, and biochemistry* 59:1498-1502
522 Hu Y, Catchmark JM, Zhu Y, Abidi N, Zhou X, Wang J, & Liang N (2014) Engineering of
523 porous bacterial cellulose toward human fibroblasts ingrowth for tissue engineering.
524 *Journal of Materials Research* 29:2682-2693
525 Ishikawa A, Matsuoka M, Tsuchida T, & Yoshinaga F (2014) Increase in cellulose
526 production by sulfaguanidine-resistant mutants serived from *Acetobacter xylinum*
527 subsp.*sucrofermentans*. *Bioscience, biotechnology, and biochemistry* 59:2259-2262
528 Jagannath A, Manjunatha SS, Ravi N, & Raju PS (2011) The effect of different substrates
529 and processing conditions on the textural characteristics of bacterial cellulose (*Nata*)
530 produced by *Acetobacter xylinum*. *Journal of Food Process Engineering* 34:593-608
531 Keshk S, & Sameshima K (2006) Influence of lignosulfonate on crystal structure and
532 productivity of bacterial cellulose in a static culture. *Enzyme and Microbial*
533 *Technology* 40:4-8
534 Lin S-B, Hsu C-P, Chen L-C, & Chen H-H (2009) Adding enzymatically modified gelatin to
535 enhance the rehydration abilities and mechanical properties of bacterial cellulose.
536 *Food Hydrocolloids* 23:2195-2203
537 Lopez-Sanchez P, Cersosimo J, Wang D, Flanagan B, Stokes JR, & Gidley MJ (2015)
538 Poroelastic mechanical effects of hemicelluloses on cellulosic hydrogels under
539 compression. *PLoS One* 10:e0122132
540 Lopez-Sanchez P, Rincon M, Wang D, Brulhart S, Stokes JR, & Gidley MJ (2014)
541 Micromechanics and Poroelasticity of Hydrated Cellulose Networks.
542 *Biomacromolecules* 15:2274-2284
543 Martínez-Sanz M, Lopez-Sanchez P, Gidley MJ, & Gilbert EP (2015) Evidence for
544 differential interaction mechanism of plant cell wall matrix polysaccharides in
545 hierarchically-structured bacterial cellulose. *Cellulose* 22:1541-1563
546 Martínez-Sanz M, Mikkelsen D, Flanagan B, Gidley MJ, & Gilbert EP (2016) Multi-scale
547 model for the hierarchical architecture of native cellulose hydrogels. *Carbohydrate*
548 *Polymers* 147:542-555
549 McKenna BA, Mikkelsen D, Wehr JB, Gidley MJ, & Menzies NW (2009) Mechanical and
550 structural properties of native and alkali-treated bacterial cellulose produced by
551 *Gluconacetobacter xylinus* strain ATCC 53524. *Cellulose* 16:1047-1055
552 Mikkelsen D, Flanagan BM, Wilson SM, Bacic A, & Gidley MJ (2015) Interactions of
553 arabinoxylan and (1,3)(1,4)-beta-glucan with cellulose networks. *Biomacromolecules*
554 16:1232-1239

555 Nakayama A, Kakugo A, Gong JP, Osada Y, Takai M, Erata T, & Kawano S (2004) High
556 mechanical strength double-network hydrogel with bacterial cellulose. *Advanced*
557 *Functional Materials* 14:1124-1128
558 Quero F, Nogi M, Yano H, Abdulsalami K, Holmes SM, Sakakini BH, & Eichhorn SJ (2010)
559 Optimization of the mechanical performance of bacterial cellulose/poly(L-lactic) acid
560 composites. *ACS Applied Materials & Interfaces* 2:321-30
561 Ruka DR, Simon GP, & Dean KM (2012) Altering the growth conditions of
562 *Gluconacetobacter xylinus* to maximize the yield of bacterial cellulose. *Carbohydrate*
563 *Polymers* 89:613-622
564 Shoda M, & Sugano Y (2005) Recent advances in bacterial cellulose production.
565 *Biotechnology and Bioprocess Engineering* 10:1-8
566 Son H-J, Kim H-G, Kim K-K, Kim H-S, Kim Y-G, & Lee S-J (2003) Increased production of
567 bacterial cellulose by *Acetobacter* sp. V6 in synthetic media under shaking culture
568 conditions. *Bioresource Technology* 86:215-219
569 Stokes JR (2012) Food materials science and engineering. In Bhandari B, & Roos YH (Eds.),
570 *Food biopolymer gels, microgel and nanogel structures, formation and rheology* (pp.
571 151-176). New Jersey:Wiley-Blackwell.
572 Tokoh C, Takabe K, & Fujita M (2002) Cellulose synthesized by *Acetobacter xylinum* in the
573 presence of plant cell wall polysaccharides. *Cellulose* 9:65-74
574 Ullah H, Santos HA, & Khan T (2016) Applications of bacterial cellulose in food, cosmetics
575 and drug delivery. *Cellulose* 23:2291-2314
576 Watanabe K, Tabuchi M, Ishikawa A, Takemura H, Tsuchida T, Morinaga Y, & Yoshinaga F
577 (1998) *Acetobacter xylinum* mutant with high cellulose productivity and an ordered
578 structure. *Bioscience, biotechnology, and biochemistry* 62:1290-1292
579 Whitney SEC, Gothard MGE, Mitchell JT, & Gidley MJ (1999) Roles of cellulose and
580 xyloglucan in determining the mechanical properties of primary plant cell walls. *Plant*
581 *Physiology* 121:657-664
582 Zhang J, Yang Y, Deng J, Wang Y, Hu Q, Li C, & Liu S (2017) Dynamic profile of the
583 microbiota during coconut water pre-fermentation for *nata de coco* production. *LWT -*
584 *Food Science and Technology* 81:87-93

585

Highlights

1. Cellulose hydrogel mechanical properties differed with *Komagataeibacter* strain used.

2. Hydrogel properties depended on both cellulose concentration and network structure.

3. Compression caused fibre coalescence, reducing network relaxation and water movement.

4. Textural variation in hydrogels achieved by strain selection and/or post-synthesis compression.